



Royal Netherlands Institute for Sea Research

This is a pre-copyedited, author-produced version of an article accepted for publication, following peer review.

Duyck, E. & de Jong, M.F. (2021). Circulation over the South-East Greenland Shelf and potential for liquid freshwater export: a drifter study. *Geophysical Research Letters*, 48: e2020JB020886.

Published version: <https://doi.org/10.1029/2020gl091948>

NIOZ Repository: <http://imis.nioz.nl/imis.php?module=ref&refid=334005>

Research data: <https://doi.org/10.25850/nioz/7b.b.4>

[Article begins on next page]

The NIOZ Repository gives free access to the digital collection of the work of the Royal Netherlands Institute for Sea Research. This archive is managed according to the principles of the [Open Access Movement](#), and the [Open Archive Initiative](#). Each publication should be cited to its original source - please use the reference as presented.

When using parts of, or whole publications in your own work, permission from the author(s) or copyright holder(s) is always needed.

Circulation over the South-East Greenland Shelf and Potential for Liquid Freshwater Export: a Drifter Study

E. Duyck¹, M.F. De Jong¹

¹ NIOZ, Royal Netherlands Institute for Sea Research, Department of Ocean Systems, Texel,
The Netherlands

Corresponding author: Elodie Duyck elodie.duyck@nioz.nl

Key Points:

- Drifter tracks show steering from shelfbreak towards the EGCC at Sermilik Trough and exchanges between the EGC and EGCC downstream.
- West of Cape Farewell, drifters in the EGC and EGCC are redistributed into a shelfbreak core and a slow, eddying inner-shelf flow.
- Five of 15 shallow drifters were exported, mainly near Cape Farewell. Cold water leakage is observed from SST data in the same area.

Abstract

Freshwater input into deep convection regions could affect the overturning circulation. With a set of 15 CARTHE and 15 SVP drifters, we investigate the circulation over the south-east Greenland shelf and the potential for off-shelf freshwater export. Part of the East Greenland Current flow is steered into the East Greenland Coastal Current immediately upstream of Sermilik Trough. Between the trough and Cape Farewell, two separate cores are visible. Just past Cape Farewell drifters are redistributed into a shelfbreak core and a slow eddying shelf flow. A coastal core is reestablished downstream. Exchanges between the shelfbreak and coastal flows take place both on the east and west Greenland shelf, allowing fresher water to be diverted away from the coast. Five of 15 shallower CARTHE drifters were exported, mainly at Cape Farewell. CARTHE motion shows a higher correlation with local winds, which are more favorable for off-shelf transport in this area.

Plain Language Summary

The Atlantic Meridional Overturning Circulation is a key element of the climate system. Global warming causes an influx of freshwater over the east Greenland shelf, that could affect the Atlantic circulation if it is exported into areas where deep water is formed. We deployed 30 surface drifters in August 2019, which we combine here with existing drifter and satellite data to describe the circulation over the south-east Greenland shelf. The export of five shallow water drifters into the Irminger Sea suggests that wind could be a driver for freshwater export away from the shelf.

34 **1 Introduction**

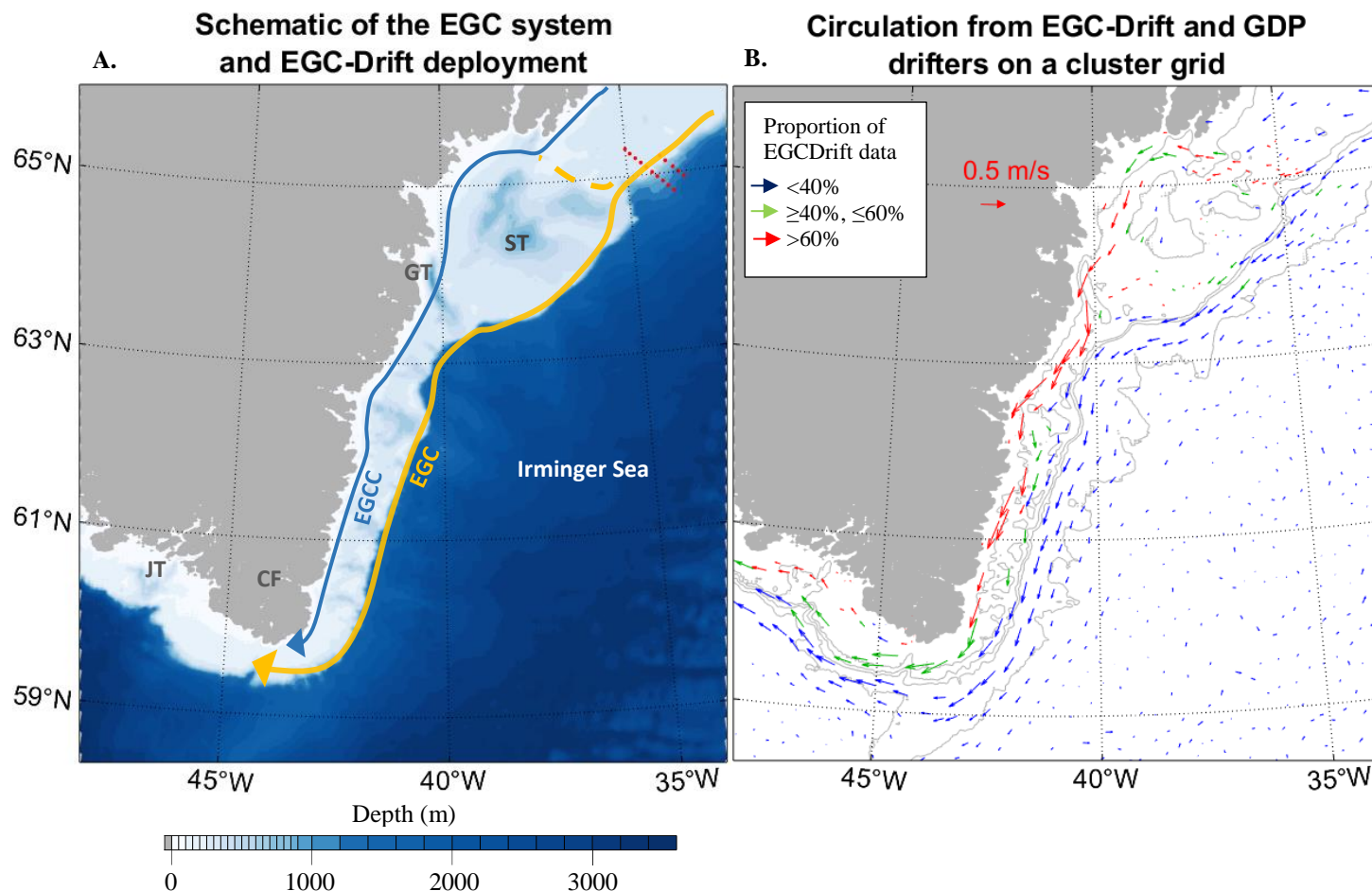
35 Atmospheric and oceanic warming of the Arctic and Subarctic regions results
36 in enhanced Greenland Ice Sheet melt and freshening of the Arctic Ocean, leading to increased
37 discharge of freshwater into the East Greenland Current (EGC) (Bamber et al., 2018; Haine et al.,
38 2015). Additional freshwater input into the convective regions of the Subpolar North Atlantic
39 could strengthen watercolumn stratification and weaken deep mixing (Aagaard & Carmack, 1989),
40 in turn affecting the strength of the Atlantic Meridional Overturning Circulation (Bakker et al.,
41 2016; Böning et al., 2016; Manabe & Stouffer, 1994). Recent findings argue for a more important
42 role of the overturning east of Greenland (Lozier et al., 2019), highlighting the particular climatic
43 importance of freshwater export from the east Greenland Shelf. This study investigates the fate of
44 liquid freshwater from the EGC system, notably potential export into the deep convection region
45 of the central Irminger Sea (de Jong et al., 2018).

46 South of Denmark Strait (DS), the EGC system (Figure 1A) consists of a main branch located at
47 the shelf-break (EGC), and a coastal branch referred to as the East Greenland Coastal Current
48 (EGCC). The EGC is found at the front between the colder, fresher waters flowing south from
49 Fram Strait and the warmer, saltier Irminger Current waters. The EGCC (Malmberg, 1967; Bacon,
50 2002) is a fresh (practical salinity < 34), 20 km-wide, surface-intensified current, with a high-
51 velocity core (speeds > 1 m s⁻¹) carrying arctic waters and Greenland runoff equatorwards (Bacon
52 et al., 2014; le Bras et al., 2018). Recent work (Foukal et al., 2020) showed that the EGCC extends
53 along the whole east Greenland coast, while confirming that deep troughs south of Denmark strait
54 divert part of the EGC into the coastal current (Sutherland & Pickart, 2008; Sutherland &
55 Cenedese, 2009). Past Cape Farewell (CF), the EGC and EGCC were first thought to merge into
56 the West Greenland Current (WGC) (Bacon, 2002), but more recent studies argue that the EGCC
57 keeps its identity as a coastal core to become the West Greenland Coastal Current (WGCC) (Lin
58 et al., 2018).

59 The cold and fresh Polar Surface Water found over most of the east Greenland shelf (Rudels et al.,
60 2002) is isolated from interior seas by the sharp hydrographic front associated with the EGC. It is
61 pushed towards the coast by the onshore Ekman transport caused by south-westward barrier winds
62 (Moore & Renfrew, 2005). However, the complex bathymetry of the shelf, meandering of the
63 front, wind strength and variability, create opportunities for export of surface waters towards the
64 interior seas, notably at CF (Holliday et al., 2007). While export of fresh waters from the west
65 Greenland shelf into the Labrador Sea is already well documented (Schulze Chretien & Frajka-
66 Williams, 2018; Wolfe & Cenedese, 2006), there is still little insight into surface water export
67 from the east Greenland shelf into the Irminger Sea.

68 Despite renewed interest in the EGC system, our understanding of the liquid freshwater circulation
69 over the east Greenland shelf remains sparse. Insight into the properties and structure of the EGC
70 is provided by synoptic sections, mooring arrays in select locations and isolated drifters (Bacon
71 2002, Reverdin 2003). In this study, we present a set of 30 drifters deployed at the east Greenland
72 continental shelf-break at approximately 65°N. Drifter deployments and data processing are

73 described in Section 2. Drifter trajectories and insights from additional datasets are presented in
 74 Section 3. Section 4 discusses the results and possible implications for liquid freshwater export.
 75
 76



77
 78 **Figure 1:**
 79 Schematic of the surface circulation over the east Greenland shelf with drifter deployment
 80 location and drifter data overview: **A.** EGC System, and main topographic features. EGC: East
 81 Greenland Current, EGCC: East Greenland Coastal Current, ST: Sermilik Trough, GT:
 82 Gyldenlove Trough, CF: Cape Farewell, JT: Julianehåb Trough; Drifters were deployed at two
 83 shelfbreak sections at 65°N (red dots). **B.** Circulation inferred from the Global Drifter Program
 84 and our EGC-DrIFT datasets combined on a cluster grid (see methods in Section 2). Arrows are
 85 colored depending on the percentage of EGC-DrIFT data in each cluster as defined in the legend.
 86 Isobaths (in grey) are drawn at 2000, 1000, 500 and 200 m depth.
 87

88 2 Materials and Methods

89 We present the first results from the East Greenland Current Drifter Investigation of Freshwater
 90 Transport (EGC-DrIFT) campaign. This study aims to elucidate possible pathways for freshwater
 91 exchanges east of Greenland with surface drifter deployments planned in the summers of 2019,

92 2020 and 2021. The dataset discussed here consists of two types of drifters. Surface Velocity
93 Program (SVP) drifters are composed of a spherical buoy and a holey sock drogue centred at 15
94 m below sea level (Lumpkin et al., 2017). Two models of SVP drifters are used: SVP-T, fitted
95 with a temperature sensor measuring sea surface temperature (SST) at 0.5 m depth, and SVP-S
96 fitted with an additional conductivity sensor to measure salinity. GPS positions and data are
97 transmitted to shore via iridium at hourly intervals for SVP-T drifters and 3-hourly intervals for
98 SVP-S drifters. CARTHE drifters (Consortium for Advanced Research for the Transport of
99 Hydrocarbon in the Environment, Novelli et al., 2017) are shallower drifters, composed of a
100 floating torus sitting low above water and a drogue at 0.4 m depth. They provide GPS tracking at
101 3-hourly intervals.

102 In total, 15 CARTHEs and 15 SVPs (seven SVP-Ts, eight SVP-Ss) were deployed along two lines
103 perpendicular to the shelf-break and 40 km apart (Figure 1A) on the 14th August 2019. The
104 southern line extended from 1200 to 250 m depth and the northern line from 1300 to 250 m depth.
105 Drifters were released 9 km apart, in pairs of one SVP and one CARTHE drifter, as to elucidate
106 the behaviour of different extents of the surface water layer. We present here their trajectories until
107 1st December 2019 and up to 48°W.

108 One SVP drifter stopped working upon launch, but the remaining 14 functioned properly. By the
109 1st December 2019, 12 SVPs and four CARTHEs (that have a shorter expected lifetime) were still
110 active. SVP-Ts occasionally (4% of dataset) display repeated positions, mostly corresponding to
111 one to two hours GPS gaps. SVP-Ss do not experience similar issues. CARTHEs display GPS gaps
112 that can last for several days. Temperature and conductivity timeseries are despiked and other
113 hydrographic properties, such as absolute salinity and density are derived using the TEOS10
114 toolbox (Mc Dougall and Barker, 2011). Drifter velocities, computed from displacement, are
115 filtered with a 25-hour centered Butterworth filter to remove high-frequency components. The
116 presence of the drogues on SVP drifters is monitored from a submergence sensor and the time to
117 first GPS fix, both of which exhibit drastic changes when a drogue is lost. No SVP drifter seems
118 to have lost its drogue before 1st December 2019. Finally, the dataset is resampled using linear
119 interpolation on a 3-hour regular grid, not interpolating data gaps longer than 12h.

120 We use the Global Drifter Program (GDP) quality-controlled 6-hour interpolated dataset (Lumpkin
121 & Centurioni, 2019) to contextualize our results. GDP and EGC-DrIFT data are non-uniformly
122 distributed in the region, and therefore less suitable for regular spatial gridding. Instead, we
123 combine EGC-DrIFT and GDP drifter data on an irregular grid built with a clustering method
124 using a k-mean algorithm. This algorithm groups neighboring observations in clusters with an
125 iterative assignment/update mechanism, in order to find a solution minimizing the distance
126 between observations and cluster centers. See McKay (2003) for more details on the algorithm, or
127 Koszalka and LaCasce (2010) for an example of its application to drifter data. We choose a k
128 number of clusters so that the mean amount of observations per cluster is 80, and do not take into
129 account clusters with less than 20 data points

130 Surface winds from 1993 to 2020 are retrieved from the ERA5 atmospheric reanalysis hourly data
131 on single levels (Copernicus Climate Change Service, 2017). Wind data are used to compute the

132 correlation coefficient between wind and drifter motion. This coefficient is the magnitude of the
 133 complex correlation between wind and drifter velocities ($u(t)+i \cdot v(t)$) (Poulain 2009). Wind data
 134 are also used to evaluate potential for off-shelf Ekman transport along the east Greenland shelf.
 135 Wind components are interpolated along the shelfbreak, defined as the 500 m isobath, and Ekman
 136 transport is computed from wind stress as:

$$138 \quad \begin{cases} U_{ek} = \frac{T_y}{f * \rho} \\ V_{ek} = \frac{-T_x}{f * \rho} \end{cases}$$

137

139 T_x , T_y being wind stress components, $\rho=1027 \text{ kg m}^{-3}$ and $f=10^{-4} \text{ s}^{-1}$. Along and across shelf Ekman
 140 transports are then derived using the local angle of the 500 m isobath, and used to compute the
 141 proportion of days with positive off-shelf Ekman transport along the shelf.

142 SST is retrieved from the GHRSSST Level 4 MUR Global Foundation SST Analysis (JPL MUR
 143 MEASUREs Project, 2015), a data blend of microwave, infrared, ice fraction and in situ
 144 measurements, with a very high resolution (1 km) in cloudless conditions (Chin et al., 2017). Cloud
 145 cover sometimes diminishes the real resolution of the MUR dataset and can cause artifacts. The
 146 quality of the MUR SST data at times of interest is verified by comparing it to the GHRSSST Level
 147 4 OSTIA Global Foundation SST Analysis (UK MetOffice, 2012).

148 **3 Results**

149 The trajectories of the EGC-DrIFT SVP buoys are consistent with existing GDP trajectories, while
 150 providing extended coverage close to the coast and a denser sampling of the circulation over the
 151 shelf (Figure 1B). Although the EGC-DrIFT drifters are limited in numbers they close an important
 152 data gap in the inner shelf region and provide coverage of the EGC and EGCC simultaneously,
 153 allowing comparison of properties and insight into exchanges taking place between these two
 154 cores.

155 The drifters take one to two months to reach the southern tip of Greenland. They quickly separate
 156 into three groups after deployment (figures 2B and 2C): 1) following the EGC, 2) steering around
 157 Sermilik Trough (ST) into the EGCC, and 3) entering the trough before joining the EGCC.

158 The first group follows the EGC and is composed of 12 drifters, among those deployed the furthest
 159 offshore (seven out of 15 (7/15) CARTHEs and 5/14 SVPs). In the EGC core, SVPs measure
 160 temperatures about 10°C and absolute salinities between 34.6 and 35.2 g kg^{-1} (Figures 2E and F).
 161 Speeds do not exceed 0.6 m s^{-1} as the EGC is steered around ST (Figure 2D). The three SVP
 162 drifters from the northern line first head offshore, but loop around and come back on the inshore
 163 side of the EGC. Three SVPs and one CARTHE re-enter the shelf at different points along the
 164 trough. Out of the core, their motion becomes very slow ($<0.1 \text{ m s}^{-1}$) and inertial. They join the
 165 EGCC just downstream of ST, measuring a sharp decrease in temperature as they enter the coastal
 166 core.

167 Ten drifters (2/15 CARTHEs, 8/14 SVP drifters) belong to the second group, which is steered
168 around ST directly towards the EGCC. They are initially slow ($<0.1 \text{ m s}^{-1}$) but accelerate as they
169 get closer to the coast, eventually reaching speeds up to 0.8 m s^{-1} as they enter the EGCC core.
170 Inside the core, they measure a large range of salinities (29 to 34 g kg^{-1}) and temperatures between
171 3 and 5.5°C , the coldest and freshest waters being closest to the coast.

172 Finally, seven drifters (6/15 CARTHEs and 1/14 SVPs) move across the trough before joining the
173 EGCC. They all follow similar trajectories as they flow from their deployment area, close to the
174 shelf-break, into the trough and later into the EGCC. Their speed inside the trough does not exceed
175 0.2 m s^{-1} . The SVP drifter measures temperatures around 7°C , and salinities around 34.5 g kg^{-1} in
176 the middle of ST.

177 South of ST, only two groups are identifiable, associated with the two current cores. As the
178 Greenland shelf narrows downstream of ST, drifters in the EGCC are steered along the Gyldenløve
179 Trough and accelerate, reaching speeds of more than 1 m s^{-1} . The EGCC remains faster than the
180 EGC until they reach CF. The cores are well defined but exchanges take place between them. As
181 was previously observed with a CTD section by Sutherland & Pickart (2008), the two cores come
182 closer together just downstream of ST, at the narrowest part of the shelf. There, four of the
183 CARTHEs are deviated from the EGCC to the EGC. Further downstream, two SVPs and one
184 CARTHE also leave the EGCC for the EGC. As the drifters near CF, seven SVPs and no CARTHE
185 remain in the EGCC, four SVPs and six CARTHEs in the EGC.

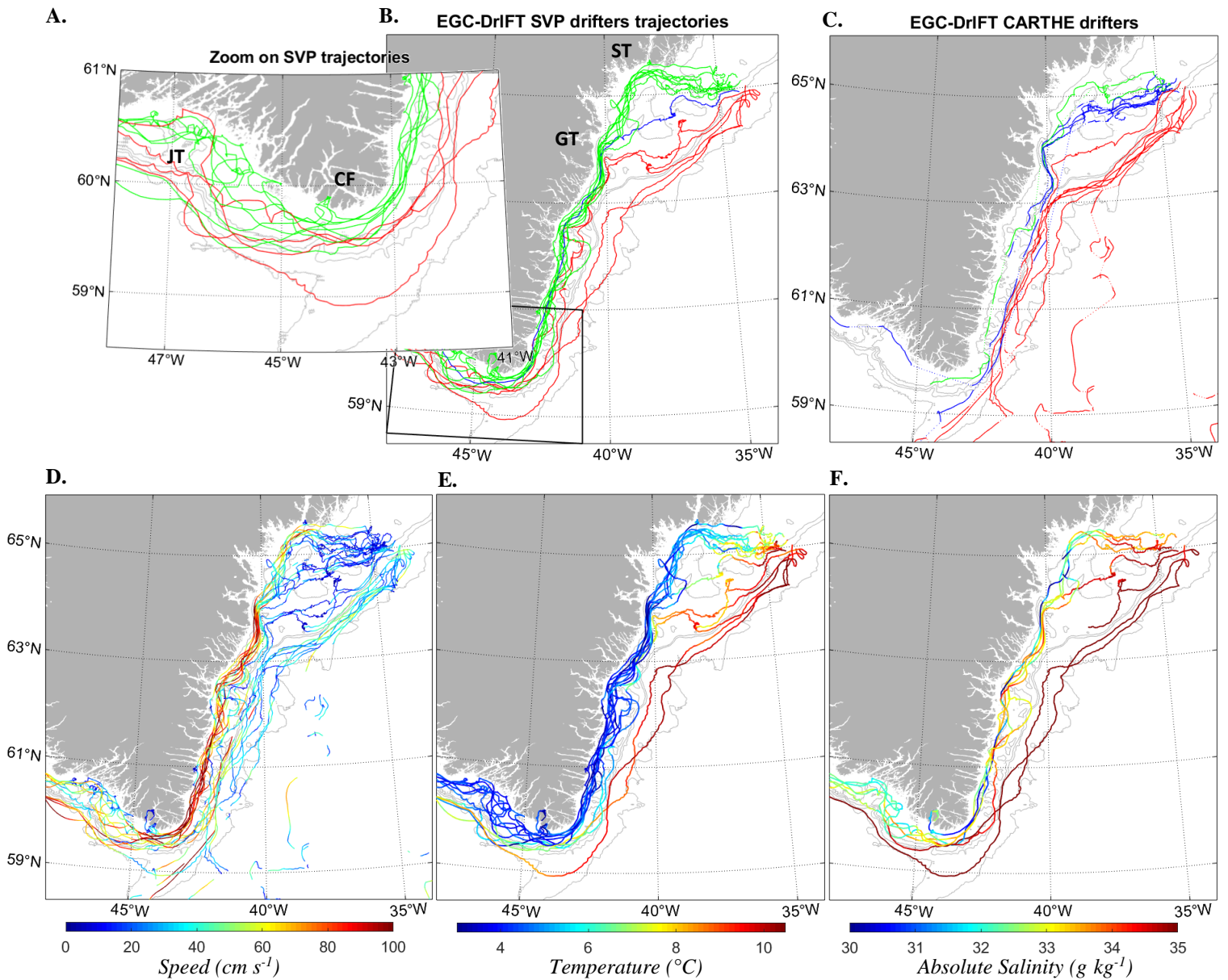
186 Four of these CARTHEs are exported into the Irminger Sea just before rounding CF. The two
187 others round the cape and enter the west Greenland shelf. Another CARTHE drifter had been
188 exported earlier at a bathymetric bend downstream of ST. The others stopped functioning.

189 West of CF, only one strong (1 m s^{-1}) velocity core is visible, at the shelf-break, with a slower, less
190 laminar flow over the shelf. As illustrated in Figure 2A, SVPs originating from the EGCC (green)
191 spread over the shelf as they round the cape. Two SVPs remain close to the shore, showing slow
192 and eddying motions, while five SVPs approach the shelfbreak, two of which enter the WGC.
193 Similarly, two of the EGC-origin SVPs (red) enter the shelf on the western side of Greenland.
194 Most shelf SVPs are then steered along Julianehåb Trough. This redistribution of coastal and
195 shelfbreak floats suggests that the WGC and WGCC are not as clearly separated as the EGC and
196 EGCC, enhancing potential for freshwater exchange away from the inner shelf west of CF.

197

198

199



200

201

Figure 2:

203 Overview of drifter trajectories and along-track properties. A. Zoom on SVP trajectories at CF,
 204 distinguishing origin from the EGC (red) and EGCC (green) B. SVP trajectories, coloured in
 205 three groups (EGCC: green, ST: Blue, EGC: Red); ; C. Same as B for CARTHEs; D. Drifter
 206 speed in cm s^{-1} ; E. Temperature in $^{\circ}\text{C}$ from SVP-S and SVP-Ts; F. Absolute salinity from SVP-
 207 Ss in g kg^{-1} . Isobaths (in grey) are drawn at 2000, 1000, 500 and 200 m depth.

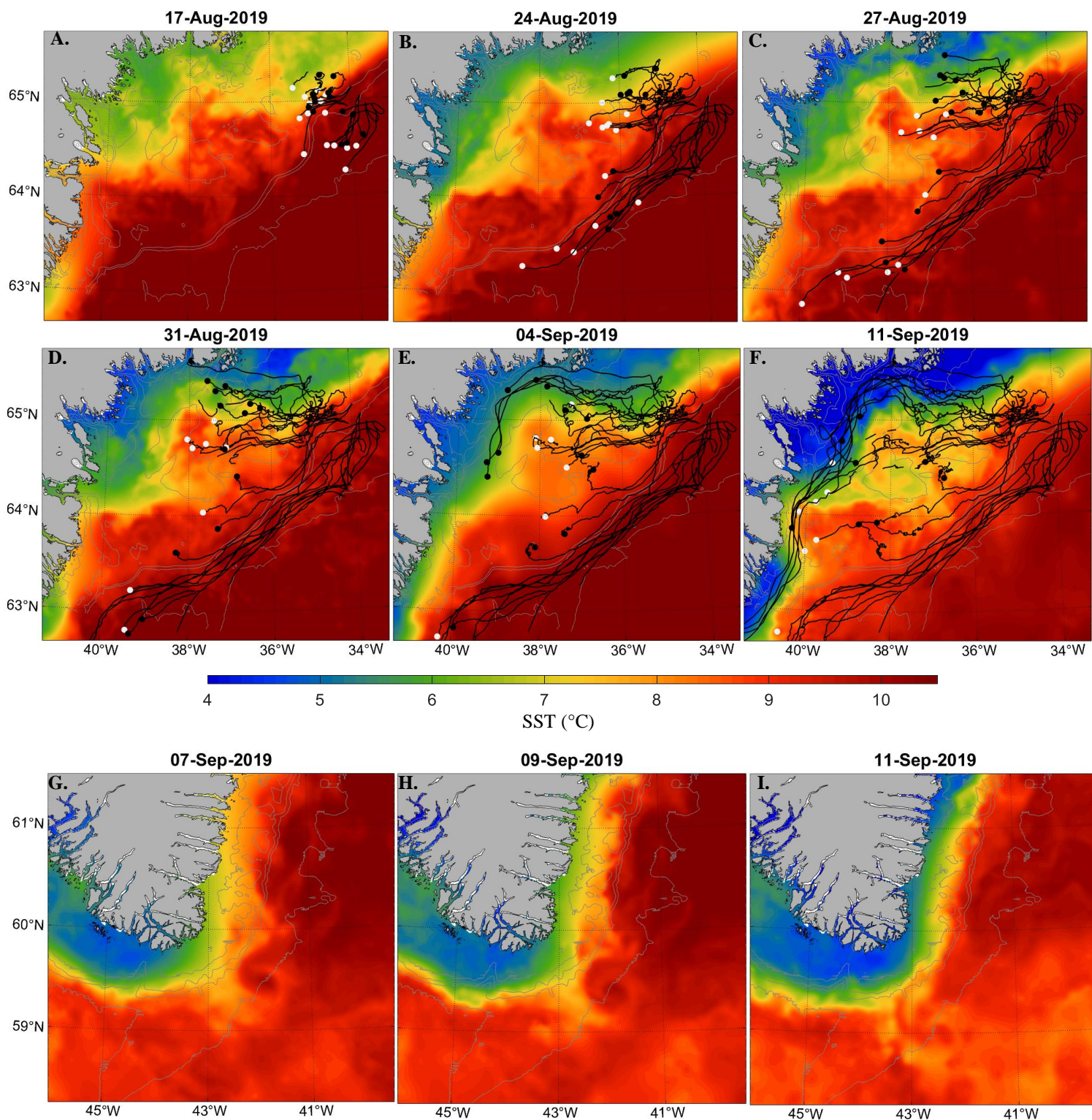
208

209

210 CARTHE and SVP drifters display different behaviours: As they approach ST, nearly all SVPs
211 join either the EGC or the EGCC, when nearly half of the CARTHEs cut across the trough. A
212 majority of CARTHEs remain in or re-enter the EGC when most SVP drifters are part of the
213 EGCC. Most of the exchanges between the EGC and EGCC cores, and all the export into the
214 Irminger Sea, are observed with CARTHE drifters. Though CARTHEs and SVPs are both built to
215 minimize wind drag and have similar water following capabilities (Novelli et al, 2017), CARTHEs
216 have shallower anchors (0.4 m against 15 m), and are therefore more directly influenced by wind
217 forcing. This is confirmed by computing the correlation between drifter and wind velocities,
218 reaching 0.66 for CARTHEs, against 0.23 for SVPs, a value that is consistent with existing studies
219 (Poulain 2009).

220 Drifter data are limited in space and time and therefore only provide a limited overview of
221 processes at the front. We investigate the correspondence between very-high resolution satellite
222 SST measurements (1 km) and drifter tracks to assess the use of satellite SST as a source of
223 information for surface circulation over the shelf when no drifter data is available. The SST
224 snapshots (Figure 3A-F) show the concurrent evolution of drifter tracks and MUR SST at ST, from
225 deployment until the beginning of September. Two temperature fronts are visible in the snapshots,
226 which coincide well with the EGC and EGCC as inferred from drifter tracks. Drifters that move
227 across ST closely follow warm water entering the trough from the north-east (24th - 27th August).
228 South of the trough, a second warm-water intrusion is visible, coincident with drifters from the
229 EGC re-entering the shelf (4th-11th September). Both SVPs and CARTHEs trajectories are
230 consistent with the MUR SST patterns, suggesting the satellite data reflects the surface circulation
231 well. Looking at the complete MUR (2002-2020) and OSTIA (2007-2020) SST time series, we
232 repetitively find the same patterns in ST suggesting that the circulation observed with the drifters
233 is typical of the area.

234 The agreement between drifter tracks and SST patterns suggests that high resolution SST data can
235 help infer variability of the location of the front over the East Greenland shelf. We use the MUR
236 SST data to further investigate potential for freshwater export at CF. Figures 3G-I show a cold
237 water tongue exiting the shelf at CF in early September 2019. Similar features are visible at CF at
238 other times and could be markers of an export pathway for fresh and cold surface shelf waters
239 towards the Irminger Sea. Due to cloud cover at the exact time when the CARTHE drifters were
240 exported, it is not possible to investigate that specific event with the MUR SST data. Further
241 observations or model analysis are necessary to verify the link between such cold water signature
242 in the SST data and surface water export.



243

244 **Figure 3:** Sea surface temperature snapshots from MUR at ST and CF.

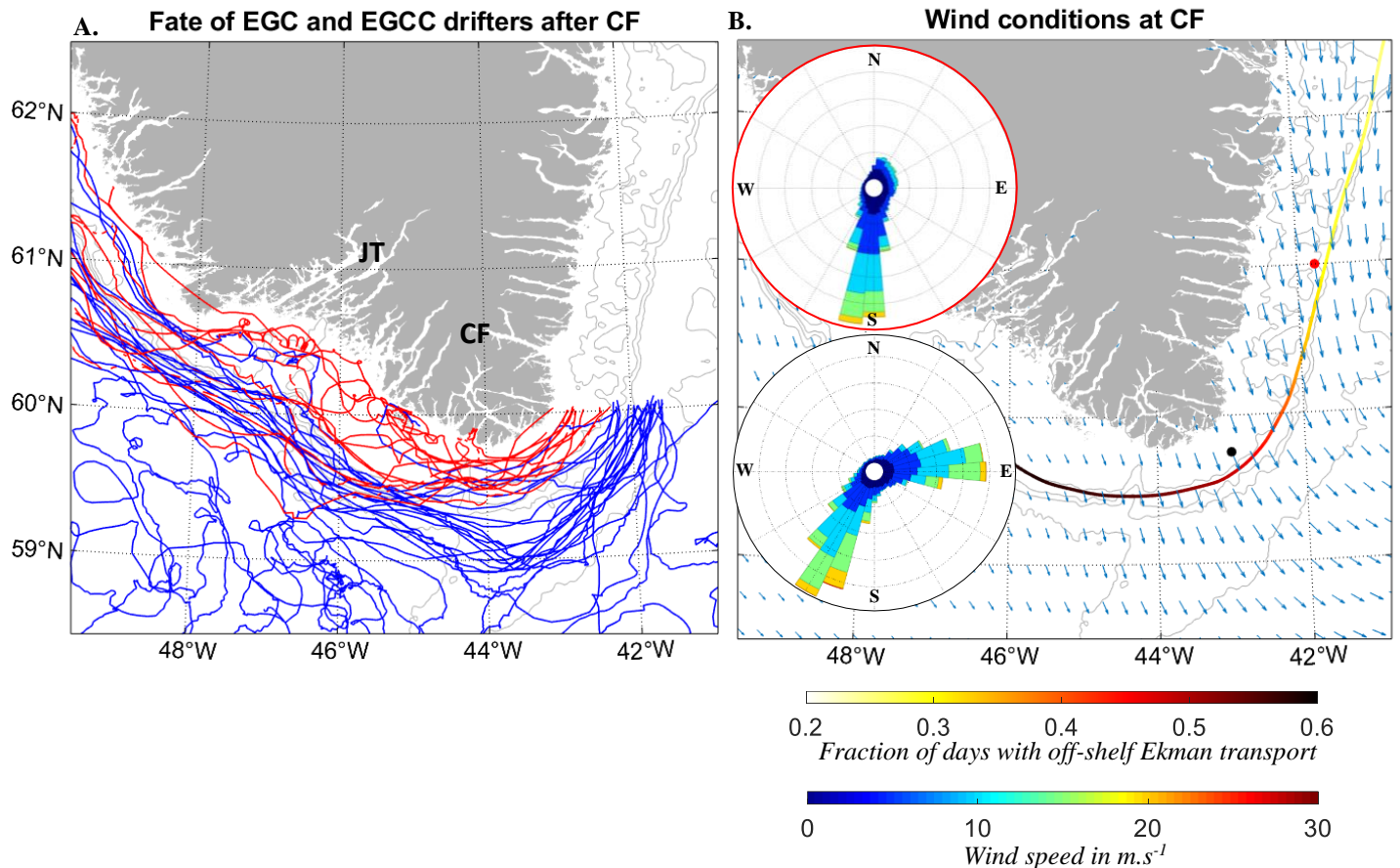
245 **A-F.** Co-evolution of SST with SVPs (Black) and CARTHEs (White) drifters from deployment
 246 through 11 September. Dots indicate drifter position at the time of the snapshots, with tracks shown
 247 since deployment. **G-I.** Instability at the EGC front at CF forming a cold water tongue, likely a
 248 marker of shelf water export. Isobaths (in grey) are drawn at 2000, 1000, 500 and 200 m depth.

249 4 Discussion and conclusion

250

251 The circulation of freshwater over the south-east Greenland shelf and its potential export into the
252 Irminger Sea are of particular climatic importance. In this study, we presented observations from
253 drifters deployed during the EGC-DrIFT campaign, in August 2019. Our results generally agree
254 with existing literature regarding the position, speed and properties of the EGC and EGCC cores
255 (Harden et al., 2014; Sutherland & Pickart, 2008), and extend existing drifter coverage closer to
256 the coast.

257 The new drifter dataset shows exchanges between the East and West Greenland shelf and
258 shelfbreak cores, suggesting that Greenland meltwater is not solely confined to the inner shelf.
259 Past CF, earlier studies suggested that the EGC and EGCC merge into the WGC (Bacon 2002).
260 Recent results (Lin et al 2018) argue that the coastal core keeps its identity to become the WGCC,
261 although local bathymetry does divert part of the flow to the outer shelf, causing loss of freshwater
262 to the WGC. In this study, coastal drifters show a stark behaviour change as they round the cape.
263 While drifters in the EGCC showed fast, nearly straight tracks, no clearly defined coastal velocity
264 core is visible between CF and 46°W. Part of the drifters from the EGCC are deviated towards the
265 outer shelf and the WGC. The drifters that stay on the inner shelf slow down substantially (Fig.
266 2D), displaying eddying or meandering motions, likely due to the widening of the shelf in this
267 area. As drifters are steered along Julianehab Trough, a well defined coastal core reappears. The
268 low velocities and meandering tracks on the inner shelf between Cape Farewell and Julianehåb
269 Trough suggest there was no coherent WGCC velocity core in this section of the shelf at the time
270 the drifters were there. Tracks from GDP drifters also do not show a coherent WGCC core in that
271 area, only downstream of Julianehab Trough (Fig. 4A). The location of the WGCC core may be
272 time variable, as could be interpreted from Pacini et al (2020). The combination of EGC-DrIFT
273 and GDP datasets (Fig. 4A) shows that most drifters originating from the EGCC (red) spread over
274 the western shelf, while most EGC-origin drifters (blue) flow along the western shelfbreak, with
275 exchanges taking place between the two. Past 48°W, the position of drifters with respect to the
276 shelfbreak is not indicative of their origin in either the EGCC or EGC. These exchanges contribute
277 to the export of freshwater from the inner shelf to the central Labrador Sea, as a well known eddy
278 shedding region is located shortly downstream (Lilly et al., 2003; Bracco et al., 2008; de Jong et
279 al., 2014).



280

281 **Figure 4**

282 Drifter tracks and wind conditions around CF. A. EGC-Drift (SVPs) and GDP drifter tracks
 283 originating from the EGC (blue) and EGCC (red) cores. B. Mean winds and fraction of days with
 284 positive off-shelf wind-driven transport (as defined in Methods, section 2). Windroses show speed
 285 and direction of winds at the red and black dots during 1993-2020. Isobaths (in grey) are drawn at
 286 2000, 1000, 500 and 200 m depth.

287 Out of 15 SVP and 15 CARTHE drifters, five CARTHEs were exported into the Irminger Sea,
 288 including four at CF. The motion of these shallow drifters is more strongly correlated with wind
 289 forcing, suggesting that wind could be a primary driver for export away from the east Greenland
 290 shelf into the Irminger Sea, similar to what Schulze Chretien and Frajka-Williams (2018) found
 291 for export off the west Greenland shelf. The fraction of days with positive off-shelf Ekman
 292 transport (as defined in Methods, section 2), shows a sharp transition to more off-shelf transport
 293 favourable conditions near CF (Figure 4B). This is both due to the bend in the shelf and to strong
 294 eastward wind events such as tip jets (Moore & Renfrew, 2005), opposed to the dominance of
 295 strong and persistent barrier winds along the eastern shelf, as shown by the wind-roses in Figure
 296 4B. Satellite SST snapshots at CF (Figure 3G-I) confirm that CF could be an enhanced export area
 297 for cold and fresh surface shelf waters. These export events could contribute to the low salinity

298 surface waters extending away from the shelf as found by Sutherland and Pickart (2008). Whether
 299 bathymetry driven instabilities, possibly related to the subsurface retroflexion of the EGC
 300 (Holliday et al, 2007), contribute these surface features is currently not clear. A more quantitative
 301 study of the wind driven cross-shelf freshwater export east of Greenland is ongoing.

302

303

304

305 **Acknowledgments and Data**

306 The EGC-DrIFT project is financially supported by the Innovational Research Incentives
 307 Scheme of the Netherlands Organisation for Scientific Research (NWO) under grant agreement
 308 nos. 016.Vidi.189.130.

309 The drifter dataset presented in this study is available at : Duyck, E., & de Jong, M.F. (2020),
 310 EGC-DrIFT drifter dataset Kulusuk deployment 2019, doi:10.25850/nioz/7b.b.4

311 We thank the captain and crew of the M/V Adolph Jansen, from which drifters were deployed.

312 **References**

313

314 Aagaard, K., & Carmack, E. C. (1989). The role of sea ice and other fresh water in the Arctic circulation. *Journal of*
 315 *Geophysical Research*, 94(C10), 14485. <https://doi.org/10.1029/JC094iC10p14485>

316 Bacon, S. (2002). A freshwater jet on the east Greenland shelf. *Journal of Geophysical Research*, 107(C7).
 317 <https://doi.org/10.1029/2001jc000935>

318 Bacon, S., Marshall, A., Holliday, N. P., Aksenov, Y., & Dye, S. R. (2014). Seasonal variability of the East
 319 Greenland Coastal Current. *Journal of Geophysical Research: Oceans*, 119(6), 3967–3987.
 320 <https://doi.org/10.1002/2013JC009279>

321 Bakker, P., Schmittner, A., Lenaerts, J. T. M., Abe-Ouchi, A., Bi, D., van den Broeke, M. R., Chan, W. L., Hu, A.,
 322 Beadling, R. L., Marsland, S. J., Mernild, S. H., Saenko, O. A., Swingedouw, D., Sullivan, A., & Yin, J.
 323 (2016). Fate of the Atlantic Meridional Overturning Circulation: Strong decline under continued warming and
 324 Greenland melting. *Geophysical Research Letters*, 43(23), 12,252–12,260.
 325 <https://doi.org/10.1002/2016GL070457>

326 Bamber, J. L., Tedstone, A. J., King, M. D., Howat, I. M., Enderlin, E. M., van den Broeke, M. R., & Noel, B.
 327 (2018). Land Ice Freshwater Budget of the Arctic and North Atlantic Oceans: 1. Data, Methods, and Results.
 328 *Journal of Geophysical Research: Oceans*, 123(3), 1827–1837. <https://doi.org/10.1002/2017JC013605>

329 Böning, C. W., Behrens, E., Biastoch, A., Getzlaff, K., & Bamber, J. L. (2016). Emerging impact of Greenland
 330 meltwater on deepwater formation in the North Atlantic Ocean. *Nature Geoscience*, 9(7), 523–527.
 331 <https://doi.org/10.1038/ngeo2740>

332 Bracco, A., J. Pedlosky, and R. S. Pickart, 2008: Eddy formation near the west coast of Greenland. *J. Phys.*
 333 *Oceanogr.*, 38, 1992–2002. <https://doi.org/10.1175/2008JPO3669.1>

334 Chin, T. M., Vazquez-Cuervo, J., & Armstrong, E. M. (2017). A multi-scale high-resolution analysis of global sea
 335 surface temperature. *Remote Sensing of Environment*, 200 (December 2016), 154–169.
 336 <https://doi.org/10.1016/j.rse.2017.07.029>

337 Copernicus Climate Change Service (C3S) (2017): ERA5: Fifth generation of ECMWF atmospheric reanalyses of
 338 the global climate . Copernicus Climate Change Service Climate Data Store (CDS), [2020-03-
 339 31], <https://cds.climate.copernicus.eu/cdsapp#!/home>

340 de Jong, M. F., Oltmanns, M., Karstensen, J., & de Steur, L. (2018). Deep Convection in the Irminger Sea Observed
 341 with a Dense Mooring Array. *Oceanography*, 31(1), 50–59. <https://doi.org/10.5670/oceanog.2018.109>

- 342 de Jong, M. F., Bower, A. S., & Furey, H. H. (2014). Two Years of Observations of Warm-Core Anticyclones in the
343 Labrador Sea and Their Seasonal Cycle in Heat and Salt Stratification, *Journal of Physical Oceanography*,
344 44(2), 427–444. <https://doi.org/10.1175/JPO-D-13-070.1>
- 345 Foukal, N. P., Gelderloos, R., Pickart, R. S., A continuous pathway for fresh water along the East Greenland shelf
346 (2020). *Science Advances*, 43(6), eabc4254. <https://doi.org/10.1126/sciadv.abc4254>
- 347 Haine, T. W. N., Curry, B., Gerdes, R., Hansen, E., Karcher, M., Lee, C., Rudels, B., Spreen, G., de Steur, L.,
348 Stewart, K. D., & Woodgate, R. (2015). Arctic freshwater export: Status, mechanisms, and prospects. *Global*
349 *and Planetary Change*, 125, 13–35. <https://doi.org/10.1016/j.gloplacha.2014.11.013>
- 350 Harden, B. E., Straneo, F., & Sutherland, D. A. (2014). Moored observations of synoptic and seasonal variability in
351 the East Greenland Coastal Current. *Journal of Geophysical Research: Oceans*, 119(12), 8838–8857.
352 <https://doi.org/10.1002/2014JC010134>
- 353 Holliday, N. P., Meyer, A., Bacon, S., Alderson, S. G., & de Cuevas, B. (2007). Retroflexion of part of the east
354 Greenland current at Cape Farewell. *Geophysical Research Letters*, 34(7), L07609.
355 <https://doi.org/10.1029/2006GL029085>
- 356 JPL MUR MEaSURES Project. 2015. GHRSSST Level 4 MUR Global Foundation Sea Surface Temperature
357 Analysis (v4.1). Ver. 4.1. PO.DAAC, CA, USA. Dataset accessed [2020-03-31]
358 at <https://doi.org/10.5067/GHGMR-4FJ04>.
- 359 Koszalka, I. M., & Lacasce, J. H. (2010). Lagrangian analysis by clustering. *Ocean Dynamics*, 60(4), 957–972.
360 <https://doi.org/10.1007/s10236-010-0306-2>
- 361 le Bras, I. A.-A., Straneo, F., Holte, J., & Holliday, N. P. (2018). Seasonality of Freshwater in the East Greenland
362 Current System From 2014 to 2016. *Journal of Geophysical Research: Oceans*, 123(12), 8828–8848.
363 <https://doi.org/10.1029/2018JC014511>
- 364 Lilly, J. M., P. B. Rhines, R. Schott, K. Lavender, J. Lazier, U. Send, and E. D'Asaro, 2003: Observations of the
365 Labrador Sea eddy field. *Prog. Oceanogr.*, 59, 75–176. <https://doi.org/10.1016/j.pocean.2003.08.013>
- 366 Lin, P., Pickart, R. S., Torres, D. J., & Pacini, A. (2018). Evolution of the Freshwater Coastal Current at the
367 Southern Tip of Greenland. *Journal of Physical Oceanography*, 48(9), 2127–2140.
368 <https://doi.org/10.1175/jpo-d-18-0035.1>
- 369 Lozier, M. S., Li, F., Bacon, S., Bahr, F., Bower, A. S., Cunningham, S. A., de Jong, M. F., de Steur, L., deYoung,
370 B., Fischer, J., Gary, S. F., Greenan, B. J. W., Holliday, N. P., Houk, A., Houpert, L., Inall, M. E., Johns, W.
371 E., Johnson, H. L., Johnson, C., ... Zhao, J. (2019). A sea change in our view of overturning in the subpolar
372 North Atlantic. *Science*, 363(6426), 516–521. <https://doi.org/10.1126/science.aau6592>
- 373 Lumpkin, R., Özgökmen, T., & Centurioni, L. (2017). Advances in the Application of Surface Drifters. *Annual*
374 *Review of Marine Science*, 9(1), 59–81. <https://doi.org/10.1146/annurev-marine-010816-060641>
- 375 Lumpkin, Rick; Centurioni, Luca (2019). Global Drifter Program quality-controlled 6-hour interpolated data from
376 ocean surface drifting buoys. NOAA National Centers for Environmental Information. Dataset.
377 <https://doi.org/10.25921/7ntx-z961>. Accessed [2020-03-31]
- 378 MacKay DJC (2003) Information theory, inference, and learning algorithms. Cambridge University Press,
379 Cambridge
- 380 Malmberg, S.-A., Gade, H.G., Sweers, H.E., 1967. Report on the second joint Icelandic–Norwegian expedition to
381 the area between Iceland and Greenland in August–September 1965. *NATO Subcommittee on Oceanographic*
382 *Research, Technical Report No. 41, Irminger Sea Project, 44 pp*
- 383 Manabe, S., & Stouffer, R. J. (1994). Multiple-Century Response of a Coupled Ocean-Atmosphere Model to an
384 Increase of Atmospheric Carbon Dioxide. *Journal of Climate*, 7(1), 5–23. [https://doi.org/10.1175/1520-](https://doi.org/10.1175/1520-0442(1994)007)
385 0442(1994)007
- 386 McDougall, T. J., & Barker, P. M. (2011). *Getting started with TEOS-10 and the Gibbs Seawater (GSW)*
387 *Oceanographic Toolbox*, 28pp., SCOR/IAPSO WG127, ISBN 978-0-646-55621-5.
- 388 Moore, G. W. K., & Renfrew, I. A. (2005). Tip jets and barrier winds: A QuikSCAT climatology of high wind speed
389 events around Greenland. *Journal of Climate*, 18(18), 3713–3725. <https://doi.org/10.1175/JCLI3455.1>
- 390 Novelli, G., Guigand, C. M., Cousin, C., Ryan, E. H., Laxague, N. J. M., Dai, H., Haus, B. K., & Özgökmen, T. M.
391 (2017). A biodegradable surface drifter for ocean sampling on a massive scale. *Journal of Atmospheric and*
392 *Oceanic Technology*, 34(11), 2509–2532. <https://doi.org/10.1175/JTECH-D-17-0055.1>

- 393 Pacini, A., and Coauthors, 2020: Mean Conditions and Seasonality of the West Greenland Boundary Current System
394 near Cape Farewell. *J. Phys. Oceanogr.*, **50**, 2849–2871, <https://doi.org/10.1175/JPO-D-20-0086.1>
- 395 Poulain, P. M., Gerin, R., Mauri, E., & Pennel, R. (2009). Wind effects on drogued and undrogued drifters in the
396 eastern Mediterranean. *Journal of Atmospheric and Oceanic Technology*, 26(6), 1144–1156.
397 <https://doi.org/10.1175/2008JTECHO618.1>
- 398 Reverdin, G., Niiler, P. P., and Valdimarsson, H., North Atlantic Ocean surface currents, *J. Geophys. Res.*, 108(C1),
399 3002, doi:10.1029/2001JC001020, 2003.
- 400 Rudels, B., Fahrbach, E., Meincke, J., Budéus, G., & Eriksson, P. (2002). The East Greenland Current and its
401 contribution to the Denmark Strait overflow. *ICES Journal of Marine Science*, 59(6), 1133–1154.
402 <https://doi.org/10.1006/jmsc.2002.1284>
- 403 Schulze Chretien, L. M., & Frajka-Williams, E. (2018). Wind-driven transport of fresh shelf water into the upper
404 30m of the Labrador Sea. *Ocean Science*, 14(5), 1247–1264. <https://doi.org/10.5194/os-14-1247-2018>
- 405 Sutherland, D. A., & Cenedese, C. (2009). Laboratory Experiments on the Interaction of a Buoyant Coastal Current
406 with a Canyon: Application to the East Greenland Current. *Journal of Physical Oceanography*, 39(5), 1258–
407 1271. <https://doi.org/10.1175/2008jpo4028.1>
- 408 Sutherland, D. A., & Pickart, R. S. (2008). The East Greenland Coastal Current: Structure, variability, and forcing.
409 *Progress in Oceanography*, 78(1), 58–77. <https://doi.org/10.1016/j.pocean.2007.09.006>
- 410 UK Met Office. 2012. GHRSSST Level 4 OSTIA Global Foundation Sea Surface Temperature Analysis (GDS
411 version 2). Ver. 2.0. PO.DAAC, CA, USA. Dataset accessed [2020-06-10] at [https://doi.org/10.5067/GHOST-](https://doi.org/10.5067/GHOST-4FK02)
412 4FK02
- 413 Wolfe, C. L., & Cenedese, C. (2006). Laboratory experiments on eddy generation by a buoyant coastal current
414 flowing over variable bathymetry. *Journal of Physical Oceanography*, 36(3), 395–411.
415 <https://doi.org/10.1175/JPO2857.1>
- 416
- 417